Journal of
Nanoscience and Nanotechnology
Vol. 10, 2885–2891, 2010

Molybdenum Interlayers for Nucleation Enhancement in Diamond CVD Growth

J. G. Buijnsters[1,*], L. Vázquez[2], R. Escobar Galindo[3], and J. J. ter Meulen[1]

[1] *Institute for Molecules and Materials (IMM), Radboud University Nijmegen, 6525 ED Nijmegen, The Netherlands*
[2] *Instituto de Ciencia de Materiales de Madrid (ICMM-CSIC), C/Sor Juana Inés de la Cruz 3, Cantoblanco, 28049 Madrid, Spain*
[3] *Centro de Micro-Análisis de Materiales (CMAM), Universidad Autónoma de Madrid, C/Faraday 3, Cantoblanco, 28049 Madrid, Spain*

The use of a 50-nm thick Mo interlayer on silicon substrates for the nucleation enhancement of microcrystalline diamond (MCD) and nanocrystalline diamond (NCD) films synthesized by hot filament chemical vapour deposition was studied. The MCD and NCD films were deposited using methane concentrations of 1% and 2%, respectively. The presence of a Mo nucleation layer enabled the formation of more uniform NCD films with reduced surface roughness (rms roughness ~40 nm for a 750-nm thick layer) and with significantly less interfacial voids due to the superior nucleation densities and surface coverage in the early stages of NCD film formation. During the initial stages of MCD film growth, the nucleation density increased by one order of magnitude as compared to uncoated silicon. As a result, much thinner MCD films with smaller surface grain sizes and, thus, reduced surface roughness could be produced as well. The presence of a Mo nucleation layer not only leads to a structural optimization of NCD and MCD films but also allows fast nucleation and film growth kinetics at relatively low substrate temperatures (~575 °C), relevant for the coating of substrate materials that do not withstand high substrate temperatures.

Keywords: Diamond, Chemical Vapour Deposition, Interlayer, Nucleation, Molybdenum.

1. INTRODUCTION

In many of today's applications, such as micro- and nano-electromechanical systems (MEMS/NEMS) and wear-resistant low friction coatings, there is a need for extremely smooth interfaces. With the rapid innovations in materials design and synthesis, the need for controlling structure and function down to the atomic scale led to multiple studies devoted to the growth and characterization of nanocrystalline diamond (NCD) and so-called ultra-nanocrystalline diamond (UNCD).[1–4] To benefit from the excellent mechanical, electrical and thermal properties of (nano)diamond, minimizing the surface roughness of these polycrystalline diamond films is a prerequisite. However, the nucleation of diamond on substrates such as silicon is rather poor and needs to be enhanced significantly in order to result in smooth, submicron thick diamond layers. Previously, it was found that the nucleation density affects the mechanical properties and thermal diffusivity in ultra-thin NCD films.[5] Moreover, an improved nucleation might lower the film surface roughness, eliminate interfacial voids and allow thinner UNCD films to be grown.[2] Finally, a higher degree of surface smoothness would also increase the strength and resistance to fracture of NCD and UNCD films.[6]

There are several substrate pretreatments that effectively increase the diamond nucleation densities by altering the topography and/or composition of the substrate surface. The most common technique is based on ultrasonic agitation in a suspension of diamond powder. After pretreatment, small diamond fragments are left on the substrate surface and might act as nucleation seeds. In this way, the diamond nucleation densities are increased by many orders of magnitude as compared to untreated substrates. Another widely applied method is the so-called Bias Enhanced Nucleation (BEN) that involves the implantation of carbon ions in the sub-surface regions and the creation of a carbide-rich surface.[7] Although fairly high nucleation densities can be obtained on electrically conductive substrates, BEN generally leads to the formation of a graphitic hydrogenated amorphous carbon layer onto which diamond is nucleated.[8] This directly influences the

*Author to whom correspondence should be addressed.

 1533-4880/2010/10/2885/007 doi:10.1166/jnn.2010.1392

adhesion and, thus, tribological performance of the diamond coating.

Only very recently the use of metal interlayers for improved control of diamond nucleation and film roughness has been studied.[2, 9] The introduction of 10 nm tungsten (W) interlayers significantly increased the diamond nucleation density, led to a lower surface roughness, eliminated interfacial voids and allowed the growth of thinner NCD films.[2] Also, a 400 nm thick titanium (Ti) interlayer proved to be successful in eliminating interfacial voids and enhancing the diamond nucleation.[9] The catalyzing effect of thin films of iron (Fe) and other transition metals such as nickel (Ni) and Ti on diamond nucleation was already mentioned by Yehoda et al.[10] The strong carbide-forming tendency of these metal elements together with the possible catalyzing effect on the creation, entrapment and redistribution of carbonaceous precursor fragments by surface diffusion might favour the diamond nucleation kinetics.[11] Note that in many earlier works, metal interlayers have already been employed effectively to improve the adhesion of diamond thin films or to suppress diffusion of the highly reactive Fe and Co in steel and hard metal substrates.[12, 13] In this study, we examine the effect of a thin molybdenum (Mo) interlayer (50 nm) on the nucleation of diamond on silicon substrates at relatively low substrate temperature. Like Ti and Fe, Mo is a relatively strong carbide former and the adhesion between CVD diamond film and molybdenum substrate is generally strong.[14, 15]

2. EXPERIMENTAL DETAILS

Molybdenum films with a thickness of 50 nm were deposited onto silicon (100) wafers by RF sputtering at 5 mbar using an argon flow of 60 sccm and an RF power of 500 W. Nano- and microcrystalline diamond films were deposited on the Mo-coated Si wafers using a home-built hot-filament chemical vapour deposition reactor. The following deposition parameters were maintained constant throughout the entire study: substrate temperature: 575 °C, filament temperature: 2200 °C, pressure: 15 mbar, filament-to-substrate distance: 8–12 mm, hydrogen flow: 300 sccm. The deposition time varied between 20 minutes and 2 hours and the methane flow was varied from 3 sccm to 6 sccm, as will be indicated for the growth experiments below. A precarburized tantalum filament coil of 0.5 mm diameter was used throughout. As a seeding pre-treatment, the uncoated and Mo-coated Si wafers were ultrasonically treated in a suspension of isopropanol and nanodiamond powder (Sigma-Aldrich, particle size <10 nm) for 1 hour, followed by a rinsing in pure isopropanol for 1 minute.

Scanning electron microscopy (SEM; JEOL JSM 6330 F) and atomic force microscopy (AFM) using Nanoscope IIIa (Veeco) equipment operating in tapping mode with silicon cantilevers (nominal radius of 10 nm) were employed to characterize the surface topography of the various samples before and after diamond nucleation and diamond film growth. Microstructural analysis of the diamond deposits is performed by micro-Raman spectroscopy using an Ar-ion laser (514.5 nm) in the 800–2000 cm^{-1} range (Renishaw System 1000) using a 50× objective with a spot size of about 2 μm. Glow discharge optical emission spectroscopy (GDOES) depth profile analysis[16] of the coatings was completed using a Horiba Jobin Yvon RF GD Profiler equipped with a 4 mm diameter anode and operating at a typical radio frequency discharge pressure of 650 Pa and power of 40 W. The chamber was cleaned by sputtering a silicon (100) sample for 20 minutes. Before every experiment the samples were flushed with argon during 60 seconds. Quantified profiles were obtained automatically using the standard Jobin Yvon QUANTUM Intelligent Quantification (IQ) software. The setup was calibrated using standard materials of known composition. The signals of N, H and O have not been taken into account for the quantitative analysis of the data, although some minor effects of these emission signals on the quantified data are the result. A collection rate of 500 points/second and a total measurement time of 150 seconds were employed to measure each sample.

3. RESULTS AND DISCUSSION

Figure 1 shows 1×1 μm^2 AFM images of the silicon wafer and Mo-coated silicon wafer without and

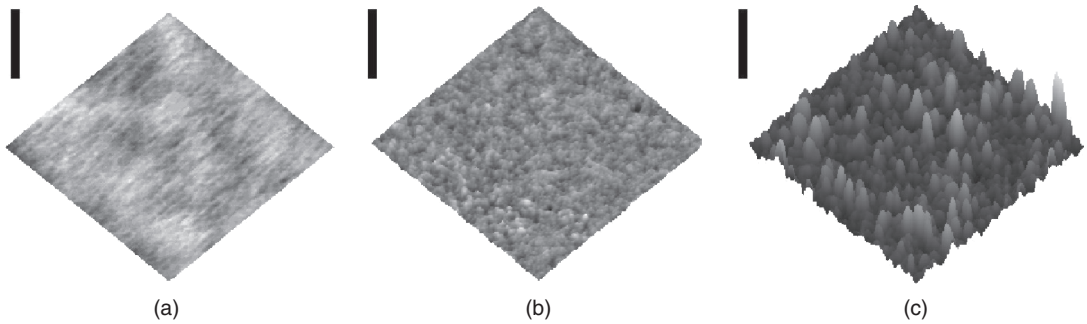

Fig. 1. 1×1 μm^2 tapping mode AFM images of the untreated silicon (a) and Mo-coated silicon without (b) and with (c) ultrasonication pretreatment in a suspension of nanodiamond powder (<10 nm) in isopropanol. The vertical bars represent 46 nm.

with ultrasonication in a nanodiamond powder suspension, respectively. The untreated silicon wafer (Fig. 1(a)) is extremely smooth and displays a root mean square (rms) roughness of 0.1–0.2 nm. The 50-nm thick Mo interlayer (Fig. 1(b)) is quite smooth, although an irregular, somewhat granular, structure of features with lateral dimensions in the range from 10 to 40 nm can be observed. The rms roughness of the Mo interlayers is in the order of 0.39–0.43 nm. To evaluate the effect of the ultrasonication seeding pre-treatment on the surface topography and roughness of the Mo-coated silicon substrates, detailed AFM analysis has been performed after ultrasonication as well. Figure 1(c) displays the Mo-coated silicon after 1 hour treatment in nanodiamond suspension and reveals a significant increase in surface rms roughness (4.4 nm) due to the presence of likely nanodiamond fragments that adhere to the surface due to van der Waals interactions.[3] The average particle density is in the order of 9×10^{10} nanoparticles/cm^2 which is close to the value derived in earlier work[3] (i.e., 1.3×10^{11} cm^{-2}) and is believed to be a lower limit for diamond nucleation as multiple nucleation can take place at a single particle and as the detected structures are likely agglomerates of diamond nanoparticles that might break up into even smaller particles by the etching effect of atomic hydrogen during the diamond CVD process.[3]

In order to study the nucleation characteristics of diamond on the pretreated silicon and Mo-coated silicon substrates, two different diamond growth series have been elaborated by varying the methane concentration from 1% to 2%. The crystalline nature of the polycrystalline layers varies from microcrystalline diamond (MCD) at 1% to nanocrystalline diamond (NCD) at 2%, as the increased methane concentration induces superior nucleation densities. As a result, relatively thin NCD layers are composed of nanometer-sized (<50 nm) diamond grains, whereas the surface grains of the MCD films, following the van der Drift regime,[17] i.e., in the complete absence of re-nucleation, continue to grow in size up to micron-sized facets.

Figure 2 shows SEM images taken at various stages of nucleation and growth of MCD films on uncoated (a–c) and Mo-coated (d–f) silicon at a substrate temperature of 575 °C. From Figures 2(a) and (d) it is clear that the diamond nucleation density after 20 minutes is significantly higher for the Mo-coated silicon substrates. Whereas the nucleation density and surface coverage for the uncoated sample are in the order of 5×10^8 cm^{-2} and 4% these are increased by at least an order of magnitude for the Mo-coated silicon (5×10^9 cm^{-2} and 54%, respectively). These differences directly influence the MCD film formation for prolonged diamond growth, as can be observed from Figures 2(b) and (e). The superior nucleation kinetics for the Mo-coated silicon lead to the formation of a continuous and closed MCD layer after only 1 hour of growth

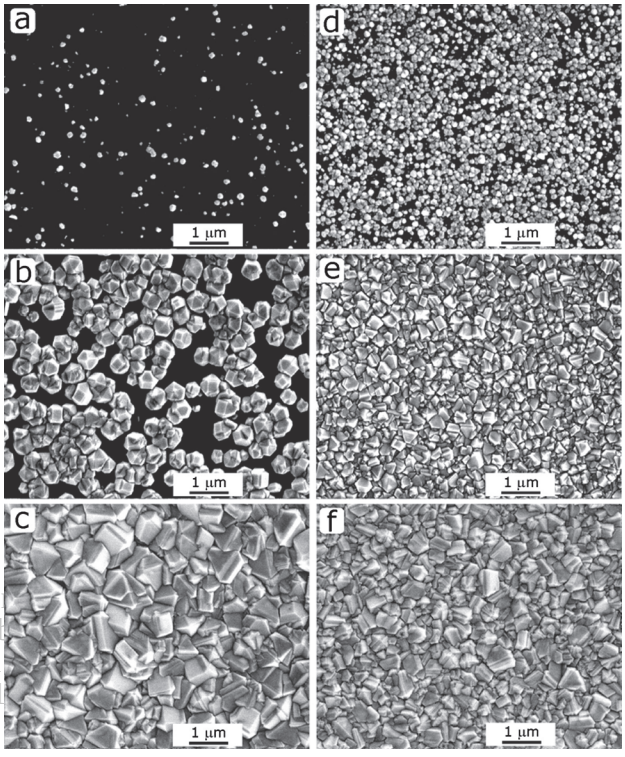

Fig. 2. Plan-view SEM images taken at various stages of the nucleation and growth of MCD films on uncoated (a–c) and Mo-coated (d–f) silicon: after 20 minutes (a, d), 1 hour (b, e) and 2 hours (c, f).

(Fig. 2(e)). On the contrary, the prolonged diamond growth on the uncoated silicon only leads to the development of partially coalesced and strongly facetted diamond grains after 1 hour (Fig. 2(b)). The formation of a continuous and closed MCD film is only observed after about 2 hours of growth (Fig. 2(c)). As a result of the higher nucleation density and earlier MCD film formation on the Mo-coated silicon, the minimal coverage thickness and rms surface roughness of the produced MCD layers are significantly reduced. For example, AFM analysis of the MCD film surfaces after 2 hours of growth shows that the rms surface roughness of the MCD film on the Mo-coated silicon sample (76 nm) is two times smaller than for the case of uncoated silicon (152 nm), the thickness being even slightly higher (2.2 μm vs. 1.8 μm, respectively).

In Figure 3 the Raman spectra of the diamond grains and MCD films grown on uncoated and Mo-coated silicon after 20 minutes and 2 hours are shown. The Raman spectrum obtained from the uncoated silicon sample exposed for 20 minutes to the diamond CVD process exhibits six clear signals, indicated by the numbers 1–6. Due to the very small quantities of diamond grains at the surface the second order signal from the silicon substrate (1: ~970 cm^{-1}) is easily observed. At 1136 cm^{-1} (2) and about 1480 cm^{-1} (5) signals related to transpolyacetylene at grain boundaries and surfaces can be distinghuished.[18] The diamond peak (3) is centred at 1333 cm^{-1} and has a

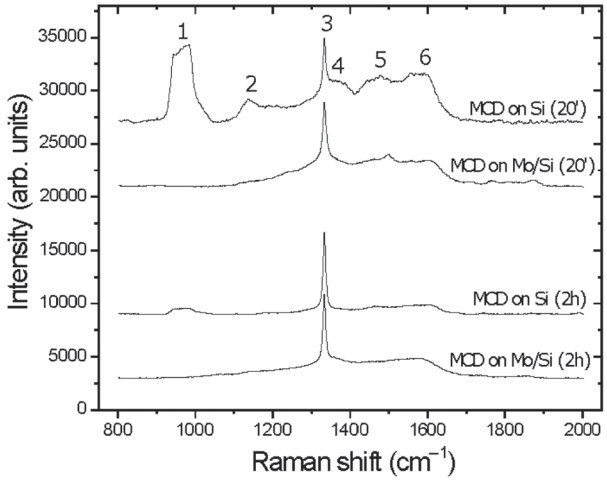

Fig. 3. Raman spectra of the diamond grains and MCD films grown on uncoated and Mo-coated silicon after 20 minutes and 2 hours. See text for the labelling of Raman signals 1–6.

full width at half maximum (FWHM) of about 9 cm^{-1}. The Raman signals of the so-called D-band (4) and G-band (6) of graphite[18] can be observed at 1365 and 1590 cm^{-1}, respectively. On the contrary, as a direct result of the superior diamond nucleation on the Mo-coated silicon the larger surface coverage results in the detection of only the diamond peak at 1333 cm^{-1} (FWHM ∼12 cm^{-1}) combined with a much lower intensity for the transpolyacetylene and graphite bands. Here, the second order signal of silicon is not observed at all. The Raman spectra of the MCD films deposited after 2 hours on both the uncoated and Mo-coated silicon substrates reveal a high film quality. A strong diamond signal is observed at 1333 cm^{-1} (FWHM ∼11 cm^{-1}), which indicates that the MCD films do not have high residual stress, and relatively low signals from non-diamond phases are detected.

In a second set of diamond growth experiments NCD films have been deposited with increased methane concentration (2%) in the applied gas mixture. Plan-view SEM images of the NCD structures formed after 20 minutes of growth on the uncoated and Mo-coated silicon substrates are shown in Figures 4(a) and (b), respectively. On the uncoated silicon the formation of coalesced clusters (∼500 nm) of NCD is observed and the surface coverage is about 65%. Clearly, when compared to the nucleation characteristics in the case of 1% methane (Fig. 2(a)), the larger NCD clusters at increased methane concentration lead to a significantly higher surface coverage, despite the nearly equal density of NCD clusters (Fig. 4(a)) and diamond nuclei (Fig. 2(a)) for both cases. Importantly, the effect of the Mo interlayer is even more pronounced. A closed and uniform NCD film is already obtained after only 20 minutes of growth. The NCD film displays a cauliflower-like surface morphology with clusters in the order of 100 nm in diameter consisting of smaller facets

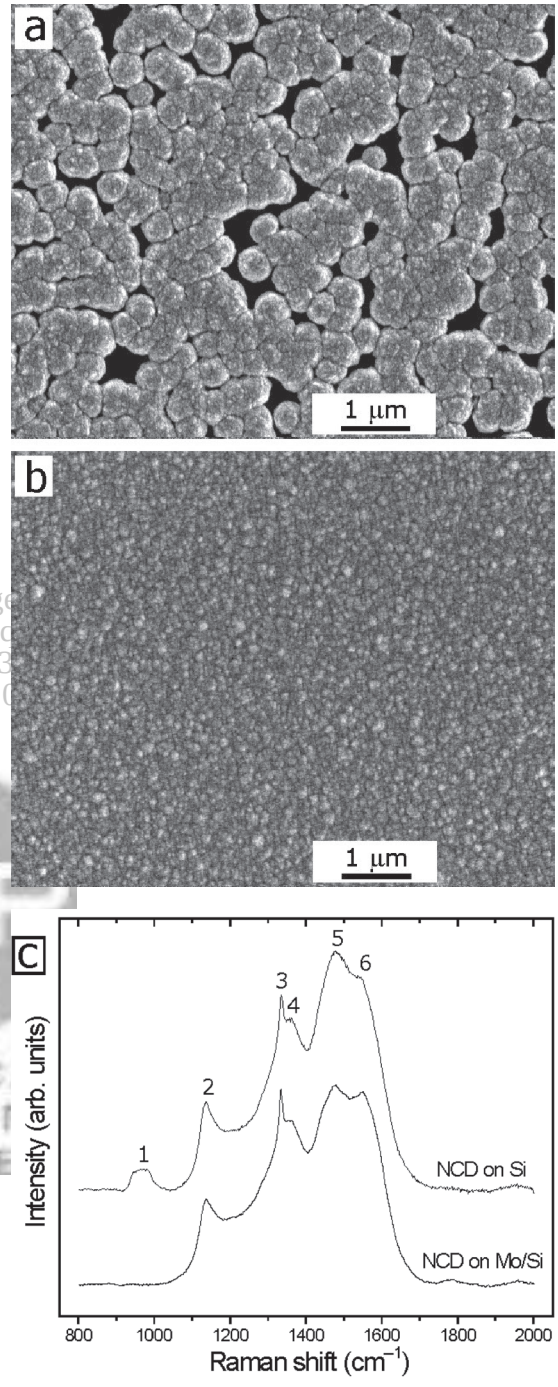

Fig. 4. Plan-view SEM images of the NCD film formation after 20 minutes on the uncoated (a) and Mo-coated (b) silicon and their corresponding Raman spectra (c). See text for labelling of Raman signals 1–6.

in the range of 15–25 nm. The Raman spectra of the NCD structures deposited on the uncoated and Mo-coated silicon substrates are shown in Figure 4(c). These highly resembling spectra reveal the characteristic Raman blueprints from NCD.[18] The six Raman peaks, which were already labelled and described for Figure 3, are visible at similar peak positions but with different relative intensities

as compared to the MCD films. Most strikingly, the intensities of the (non-diamond) features of transpolyacetylene (2, 5) and the D- and G-bands of graphite (4, 6) are increased with respect to the diamond peak. Again, the presence of the second order signal of silicon in the Raman spectra obtained from the NCD layer formed on the uncoated silicon can be ascribed to the partial surface coverage by the NCD clusters. The fine resemblance between both Raman spectra in Figure 4(c) indicates that the Mo interlayer has little to no effect on the NCD film quality.

However, the faster kinetics for the nucleation and NCD film formation in the presence of a Mo interlayer reveal large differences in NCD film thickness and film structure. In Figure 5 cross-sectional SEM images of the NCD layers deposited after 20 minutes on uncoated and Mo-coated silicon are shown. The semi-spherical NCD clusters formed on the uncoated specimen (Fig. 5(a)) are typically about 400 nm wide and 320 nm high. As a result of the non-uniform nucleation at the silicon surface, interfacial voids and open areas in-between the NCD clusters are observed. However, the NCD film grown using interfacial Mo (Fig. 5(b)) is much denser, more uniform, thicker (∼750 nm) and smoother (rms roughness ∼40 nm).

Alike the application of thin W interlayers,[2] the reduced roughness of the NCD films on Mo-coated silicon arises from the denser and more uniform nucleation. Using a 50-nm thick Mo interlayer, the vertical growth is also promoted by a factor of 2.3 as compared to the initially three-dimensional growth around fewer nucleation seeds in the case of uncoated silicon.

The 50-nm thick Mo nucleation layer can be observed clearly in Figure 5(b). While the NCD/Mo and Mo/Si interfaces reveal very sharp transitions, GDOES depth profiling has been employed to study the elemental distribution along these interfaces. In Figure 6 the compositional GDOES depth-profiles of closed NCD films deposited on uncoated and Mo-coated silicon are displayed. In the absence of any nucleation layer (Fig. 6(a)), the elemental distributions of C and Si follow a relatively smooth transition for which the individual signals interchange after a sudden, yet inexplicable, rise in carbon fraction at the very interface of NCD nucleation. The GDOES depth-profile in the presence of a Mo interlayer is much more complex (Fig. 6(b)). Here again, the carbon signal rises abruptly at the NCD/Mo interface (1) before interchanging with Si. Then, after a local minimum at (2) it shortly increases

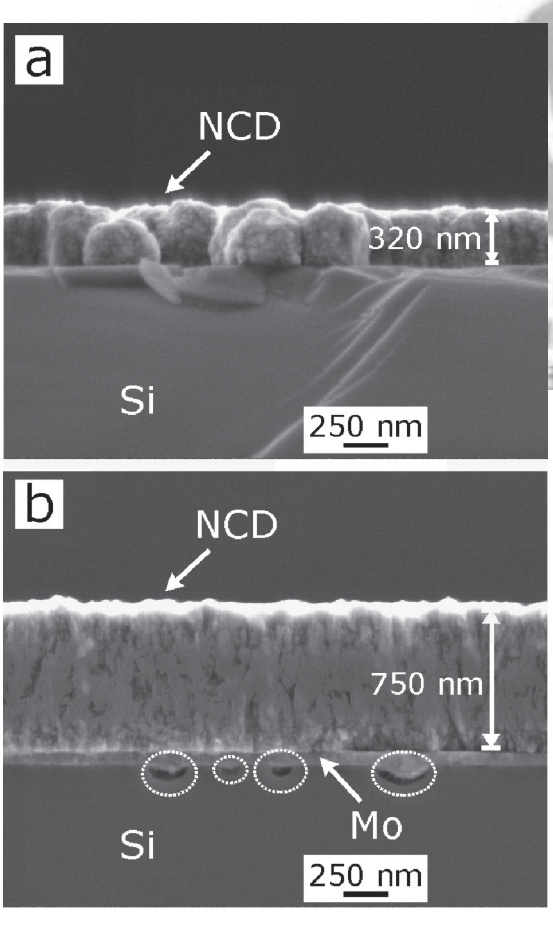

Fig. 5. Cross-sectional SEM images of the NCD films deposited after 20 minutes on the uncoated (a) and Mo-coated (b) silicon.

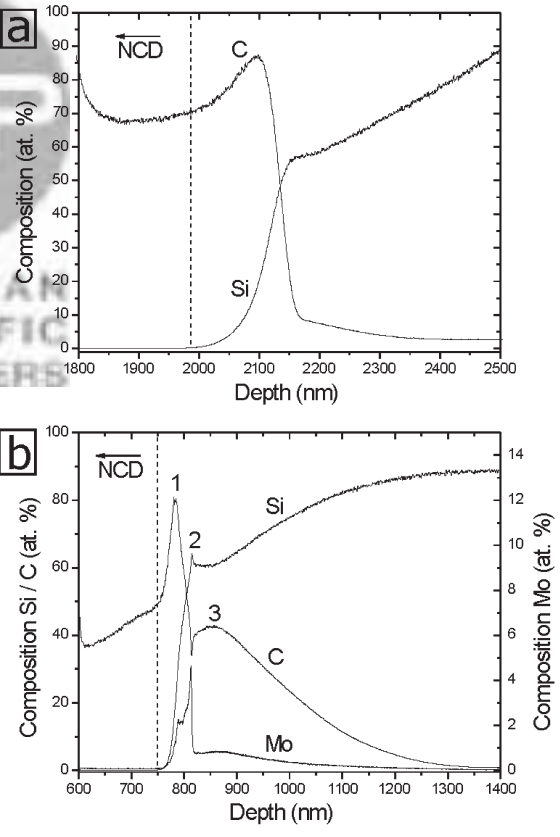

Fig. 6. Compositional GDOES depth-profiles of continuous and closed NCD films deposited on uncoated (a) and Mo-coated (b) silicon. The data are obtained from 2-μm and 750-nm thick NCD films, respectively. Please note that the NCD films extend beyond the very left-handed side of the depth scale (x-axis). See text for the labelling of 1–3 in (b).

again (3) before dropping exponentially to nearly zero bulk values. The Si signal displays a local maximum at (2) before finally displaying the general increase to maximum bulk value of the silicon substrate. It is important to notice that the transitions at (1)–(3) are observed for the Mo signal as well. The Mo signal displays a steep increase to an intermediate value at (1), an even more pronounced increase at (2), followed by a sharp drop and another local but small maximum value at (3) before exponentially dropping to zero bulk value. The observed trends indicate the formation of amorphous and/or crystalline Mo_xC and $MoSi_xC_y$ compounds within the Mo interlayer. It is known that at elevated temperatures (>300 °C) the intermixing of Mo and Si at Mo/Si interfaces leads to a phase transformation to *h*-$MoSi_2$.[19] In addition, diamond growth on molybdenum substrate materials generally results in relatively thick intermediate carbide (MoC_2) layers[14] due to the high diffusion coefficient of C in Mo and MoC_2. Consequently, the microstructure and elemental distributions within these diffusion zones in the present study are very complex and detailed TEM analysis and elemental mapping are necessary to allow a higher depth resolution in the characterization of these interlayers.

As could already be observed from Figure 5(b), voids and slight deformations of the Mo interlayer are present at the Mo/Si interface at various spots (indicated by dashed circles). Besides, the GDOES data indicate the possible formation of Mo_xC and $MoSi_xC_y$ phases and, thus, a consumption of the sputtered Mo interlayer. Therefore, we have performed a diamond growth experiment at elevated substrate temperature (750 °C) using a 1% methane gas mixture and without ultrasonication in nanodiamond powder suspension in order to study the effect of prolonged exposure to a carbon-rich environment and a higher temperature on the stability and applicability of a Mo nucleation layer. In Figures 7(a) and (b) plan-view SEM images of the surfaces of the Mo-coated silicon after 20 minutes and 2 hours are shown, respectively. After 20 minutes (Fig. 7(a)) the surface of the Mo nucleation layer has become porous and starts to rumple. Although not completely delaminated, the Mo nucleation layer suffers from severe rumpling after 2 hours (Fig. 7(b)), probably due to local adhesion failure. Besides, the diamond nucleation density is low ($\sim 1.2 \times 10^6$ cm^{-2}) and only individual, micron-sized diamond grains, which are distributed randomly on the surface, are observed. Raman spectra taken from the exposed Mo nucleation layers are demonstrated in Figure 7(c). The Raman spectrum of the sample after 20 minutes only exhibits the D- and G-bands of graphite. No Raman signal from diamond could be detected at all. However, the formation of diamond crystallites is evident after 2 hours, as a strong peak located at 1333 cm^{-1} turns up. The above analysis indicates that Mo nucleation layers without ultrasonication pre-treatment are significantly less effective at relatively high substrate temperatures (≥750 °C). Presumably, the enhanced carbon in-diffusion, carbide formation, intermixing of C, Mo and Si and, thus, molybdenum consumption are limiting the applicability of Mo nucleation layers at elevated temperatures. Proper substrate pre-treatment, such as ultrasonication with nanodiamond powder suspensions,

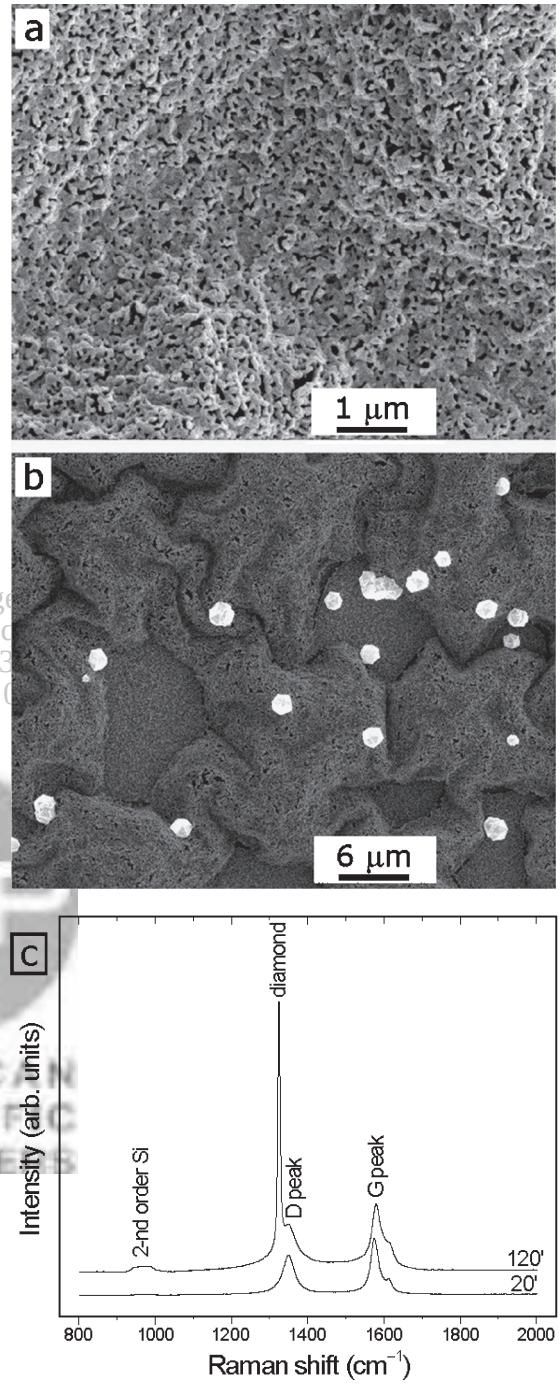

Fig. 7. Plan-view SEM images of the Mo-coated silicon after 20 minutes (a) and 2 hours (b) of exposure to the CVD growth process at elevated temperature (750 °C) and their corresponding Raman spectra (c), which were obtained after long acquisition times with multiple accumulation.

is then necessary to lead to sufficiently enhanced nucleation kinetics in order to avoid the above-mentioned problems.

4. CONCLUSIONS

In this paper we have investigated the application of a 50-nm thick Mo interlayer for the growth of MCD and NCD films. The experimental results yield the following conclusions. The use of a Mo interlayer:
(1) leads to enhanced nucleation kinetics, i.e., higher nucleation densities and surface coverage, for the growth of MCD and NCD films;
(2) reduces the fraction of interfacial voids and produces more uniform MCD and NCD layers;
(3) results in a significant reduction of the surface roughness of both MCD and NCD films;
(4) enables the synthesis of MCD and NCD films at relatively low substrate temperatures (575 °C);
(5) results in the intermixing of Mo, Si and C at elevated substrate temperatures (≥750 °C) in the case no ultrasonic substrate pretreatment step with nanodiamond powder is applied prior to the diamond CVD process. This leads to the rumpling of the Mo interlayer combined with low diamond nucleation densities.

Acknowledgments: We would like to thank M. M. J. W. van Herpen for the Mo sputtering. This research is supported by the Dutch Technology Foundation STW, applied science division of NWO and the Technology Program of the Ministry of Economic Affairs (Veni grant NAF.7527). L. Vázquez acknowledges financial support from MEC project No FIS2006-12253-C06-03.

References and Notes

1. A. V. Sumant, D. S. Grierson, J. E. Gerbi, J. Birrell, U. D. Lanke, O. Auciello, J. A. Carlisle, and R. W. Carpick, *Adv. Mater.* 17, 1039 **(2005)**.
2. N. N. Naguib, J. W. Elam, J. Birrell, J. Wang, D. S. Grierson, B. Kabius, J. M. Hiller, A. V. Sumant, R. W. Carpick, O. Auciello, and J. A. Carlisle, *Chem. Phys. Lett.* 430, 345 **(2006)**.
3. A. V. Sumant, P. U. P. A. Gilbert, D. S. Grierson, A. R. Konicek, M. Abrecht, J. E. Butler, T. Feygelson, S. S. Rotter, and R. W. Carpick, *Diamond Relat. Mater.* 16, 718 **(2007)**.
4. W. Kulisch, C. Popov, V. Vorlicek, P. N. Gibson, and G. Favaro, *Thin Solid Films* 515, 1005 **(2006)**.
5. J. Philip, P. Hess, T. Feygelson, J. E. Butler, S. Chattopadhyay, K. H. Chen, and L. C. Chen, *J. Appl. Phys.* 93, 2164 **(2003)**.
6. H. D. Espinosa, B. Peng, B. C. Prorok, N. Moldovan, O. Auciello, J. A. Carlisle, D. M. Gruen, and D. C. Mancini, *J. Appl. Phys.* 94, 6076 **(2003)**.
7. Y. Lifshitz, Th. Köhler, Th. Frauenheim, I. Guzmann, A. Hoffman, R. Q. Zhang, X. T. Zhou, and S. T. Lee, *Science* 297, 1531 **(2002)**.
8. M. M. García, I. Jiménez, O. Sánchez, C. Gómez-Aleixandre, and L. Vázquez, *Phys. Rev. B* 61, 10383 **(2000)**.
9. L.-J. Chen, N.-H. Tai, C.-Y. Lee, and I.-N. Lin, *J. Appl. Phys.* 101, 064308 **(2007)**.
10. J. E. Yehoda, R. I. Fuentes, J. C. Tsang, S. J. Whitehair, C. R. Guarnieri, and J. J. Cuomo, *Appl. Phys. Lett.* 60, 2865 **(1992)**.
11. R. Shima, Y. Chakk, and A. Hoffman, *Carbon* 38, 1839 **(2000)**.
12. J. M. Lopez, V. G. Babaev, V. V. Khvostov, and J. M. Albella, *J. Mater. Res.* 13, 2841 **(1998)**.
13. J. G. Buijnsters, P. Shankar, and J. J. ter Meulen, *Surf. Coat. Technol.* 201, 8955 **(2007)**.
14. J. G. Buijnsters, P. Shankar, W. J. P. van Enckevort, J. J. Schermer, and J. J. ter Meulen, *Thin Solid Films* 474, 186 **(2005)**.
15. M. Amar, W. Ahmed, H. Sein, A. N. Jones, and C. A. Rego, *J. Phys: Cond. Matt.* 15, S2977 **(2003)**.
16. R. E. Galindo, R. Gago, E. Forniés, A. Muñoz-Martín, A. Climent Font, and J. M. Albella, *Spectrochim. Acta Part B* 61, 545 **(2006)**.
17. A. van der Drift, *Philips Research Reports* 22, 267 **(1967)**.
18. A. C. Ferrari and J. Robertson, *Phys. Rev. B* 63, 121405 **(2001)**.
19. I. Nedelcu, R. W. E. van de Kruijs, A. E. Yakshin, and F. Bijkerk, *J. Appl. Phys.* 103, 083549 **(2008)**.

Received: 1 December 2008. Accepted: 20 January 2009.